Adsorption of indigo carmine from aqueous solution using coal fly ash and zeolite from fly ash

Terezinha E. M. de Carvalho · Denise A. Fungaro ·
Carina P. Magdalena · Patricia Cunico

Abstract Coal fly ash, a waste generated at the Figueira coal-fired electric power plant located in Brazil, was used to synthesize zeolite by hydrothermal treatment with NaOH solution at 100 °C for 24 h. The fly ash (FA) and this synthesized zeolite (ZM) that was characterized predominantly as hydroxy-sodalite were used as adsorbents for anionic dye indigo carmine from aqueous solutions. The samples were analyzed by instrumental neutron activation analysis (INAA) for the determination of As, Co, Fe, La, Mo, Na, Sb, Sc, Sm, Th, U and Zn. Effects of contact time and initial dye concentration were evaluated in the adsorption processes. The kinetics studies indicated that the adsorption followed the pseudo-second order kinetics and that surface adsorption and intraparticle diffusion were involved in the adsorption mechanism for both the adsorbents. The Langmuir isotherm model provided the best correlation of the experimental data. The maximum adsorption capacity was found to be 1.48 mg L^{-1} for FA and 1.23 mg L^{-1} for ZM. Laboratory leaching and solubilization tests conducted to classify this ZM as if was a waste residue according to the Brazilian regulation classified it as a residue non-hazardous and non-inert.

Keywords Fly ash · Zeolite synthesis · INAA · Indigo carmine · Adsorption

T. E. M. de Carvalho · D. A. Fungaro (✉) ·
C. P. Magdalena · P. Cunico
Environment and Chemistry Centre (CQMA), Nuclear and
Energy Research Institute (IPEN-CNEN/SP), Av. Professor
Lineu Prestes, 2242, São Paulo, SP CEP 05508-000, Brazil
e-mail: dfungaro@ipen.br

Introduction

Organic dyes constitute one of the larger groups of pollutants in wastewater discharged from textile and other industries. However, their discharge into water has a severe environmental impact. Among the most useful dyes, there is indigo carmine that is used as textile colouring agent, additive in pharmaceutical tablets and capsules, in confectionery items and, for medical diagnostic purposes [1, 2]. The indigo carmine is considered as a highly toxic indigoid class of dye. Contact with it can cause skin and eye irritations. It can also cause permanent injury to cornea and conjunctiva [3, 4].

Adsorption is an important technique for metals ion, color and any other pollutant removal from industrial wastewaters and radioactive wastes. The prediction of batch adsorption kinetics is necessary for the design of industrial adsorption columns [5–7].

The coal-fired power plants in the southern of Brazil produce approximately 3 Mt of ash per year, of which 65–85% is fly ash and 15–35% bottom ash. Great part of this fly ash is applied as raw material for cement and concrete production, while a small part is used in road-stabilizer, glass composites and asphalt mixtures. The remaining solid wastes are disposed in on-site ponds, nearby abandoned or active mine sites, or landfills. There is a big concern related to the non-use fly ash since is endangering surrounding surface and ground waters as it can release different and potentially toxic trace and major elements during and after its transport to the dump. Further on, leached elements are entering soils and sediments and through biosphere can enter food-chain. The coal ash in the environment is exposed to various influences, and solubilization processes take place, sometimes transforming almost insoluble metals to soluble species, and leading to pollution of water and soil [8–11].

Increasing concerns about the environmental consequences of such disposal have led to investigations into other possible utilization avenues. Furthermore, the conversion of a low-cost waste product into a higher level product would make the disposal of the remaining unused ash far more economically viable [12]. Thus continuous research is needed to develop an alternative technology for utilizing coal ashes.

Several studies have been done to demonstrate that material synthesized from coal fly ash can diminish the leachable contents of hazardous metals in polluted soils and water [13–15]. Investigations have also focused on the adsorption of organic dye compounds from waste effluent water using zeolites from coal fly ash [16–20]. These synthesized zeolites are used for the adsorption and locking up the hazardous metals, thus preventing them from leaching into the environment.

This paper aims to predict the kinetic behavior for the batch adsorption of indigo carmine dye on coal fly ash and on zeolite synthesized from this fly ash, and to verify the performance of this zeolite in locking up toxic elements when is facing the leaching and solubilization environmental conditions.

Experimental

Materials

All chemicals used in this study were of analytical grade. Indigo Carmine (IC), which was used as a model anionic dye in this work, was purchased from Vetec Química Fina Ltda and considered as purity 100%. As shown in Fig. 1, IC has two sulfonate groups, which have negative charges in aqueous solution. The general characteristics of IC are summarized in Table 1. The sample of fly ash (FA) collected in the baghouse filter was obtained from a coal-fired power plant located at Figueira County, in Paraná State, Brazil.

Zeolite synthesis

The zeolite was synthesized by hydrothermal activation of 20 g coal fly ash at 100 °C in 160 mL of 3.5 mol L^{-1} NaOH solution for 24 h [21]. The zeolitic material (ZM) was repeatedly washed with deionized water to remove
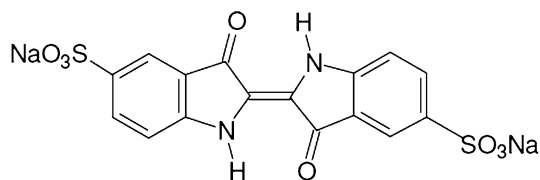
Fig. 1 Chemical structure of IC

Table 1 General characteristics of IC dye

Chemical name	Indigo carmine
Color index	73015
Chemical formula	$C_{16}H_8N_2Na_2O_8S_2$
Molar mass (g mol^{-1})	466.36
λ_{max} (nm)	610

excess sodium hydroxide until the washing water had pH $\sim$10, then it was dried at 50 °C for 24 h.

Adsorbents characterization

The FA and ZM used as adsorbents were analyzed by different techniques. Chemical composition of FA as raw material as well as ZM, in the form of major oxides, was determined by X-ray fluorescence (XRF) in a Rigaku RIX-3000 equipment. Infrared (IR) spectroscopy analysis performed with a FTIR Nexus 670 Thermo Nicolet was carried out to study their structural features. X-ray diffraction (XRD) with an automated Rigaku MiniFlex II diffractometer using Cu Kα radiation ($\lambda = 1.5405$ Å) was used to identify the main crystalline compounds. The crystalline phases present in the samples were identified with the help of ICDD (International Centre for Diffraction Data).

Adsorption studies

A stock solution was prepared in deionized water (Millipore Milli-Q) and the solutions for adsorption tests were prepared by diluting it. Concentrations of the aqueous solutions of dye were monitored on UV/Vis spectrophotometer (Varian—model Cary 1E) at 610 nm, the maximum of absorption peak of IC. The adsorption was performed using the batch procedure. Kinetic experiments were carried out by shaking 0.25 g of adsorbents with 25 mL of the IC solutions of known initial dye concentration at room temperature (25 ± 2 °C) in a shaker operated at 120 rpm. The samples were withdrawn from the shaker at different time intervals, centrifuged and the concentration in the supernatant solution was determined. For adsorption isotherms, IC solutions of different concentrations ranging from 2.8 to 23.8 mg L^{-1} were agitated with 0.25 g of FA e from 2.9 to 18.2 mg L^{-1} with the same amount of ZM, also at room temperature. The adsorption capacity (mg g^{-1}) of adsorbents was calculated using Eq. 1:

$$q_e = \frac{V(C_0 - C_e)}{M} \qquad (1)$$

where q_e is the adsorbed amount of dye per gram of adsorbent, C_0 and C_e the concentrations of the dye in the initial solution and equilibrium, respectively (mg L^{-1});

V the volume of the dye solution added (L) and *M* the amount of the adsorbent used (g).

Instrumental neutron activation analysis (INAA)

About 100 mg of FA, ZM and reference material were weighted in polyethylene bags. The accuracy of the results was determined using IAEA standard reference material SOIL-7. For irradiation, the samples, reference material and element standards were simultaneously submitted to a thermal neutron flux in the range of 3.5–5.0×10^{12} n cm^{-2} s^{-1} for 8 h at the nuclear research reactor IEA-R1 of the Nuclear and Energy Research Institute, IPEN/CNEN-SP, São Paulo, Brazil. After appropriate decay periods, γ-ray spectra of samples, reference material and element standards were measured using High-purity Ge (HPGe) detector Model POP-TOP (EG&G Ortec, Oak Ridge, TN, USA). This detector was coupled to an EG&G Ortec card and associated electronics. Spectrum analysis was carried out using VISPECT software, in TURBOBASIC language.

Leaching and solubilization tests

A ZM sample was submitted to leaching and solubilization tests for waste classification according to Brazilian regulation. The procedures for obtention of leaching extraction and for obtention of solubilized extraction of solid wastes are described at ABNT Norms [22, 23]. Ten grams of ZM sample with diameter particles with less than 9 mm were placed in a bottle and 193 mL of acetic acid solution (pH 2.88 ± 0.05) were added and agitated for 18 h at 30 rpm. After filtration with GF membrane (0.45 μm), leachable compounds were extracted, and the elements were analyzed. In the solubilization test, 100 mL of ultrapure water was added to 25 g of ZM and this suspension was agitated for 5 min and after it was allowed to stand for 7 d. After filtration, the soluble compounds were extracted and the elements were analyzed by inductively coupled plasma optical emission spectrometry (ICP-OES) in a Spectro-Flame M120 spectrometer from Spectro Analytical Instruments and by graphite furnace atomic absorption cold vapor spectrometry (GFAAS) in an Analyst 800 from Perkin-Elmer.

Results and discussion

Characterization of the adsorbents material

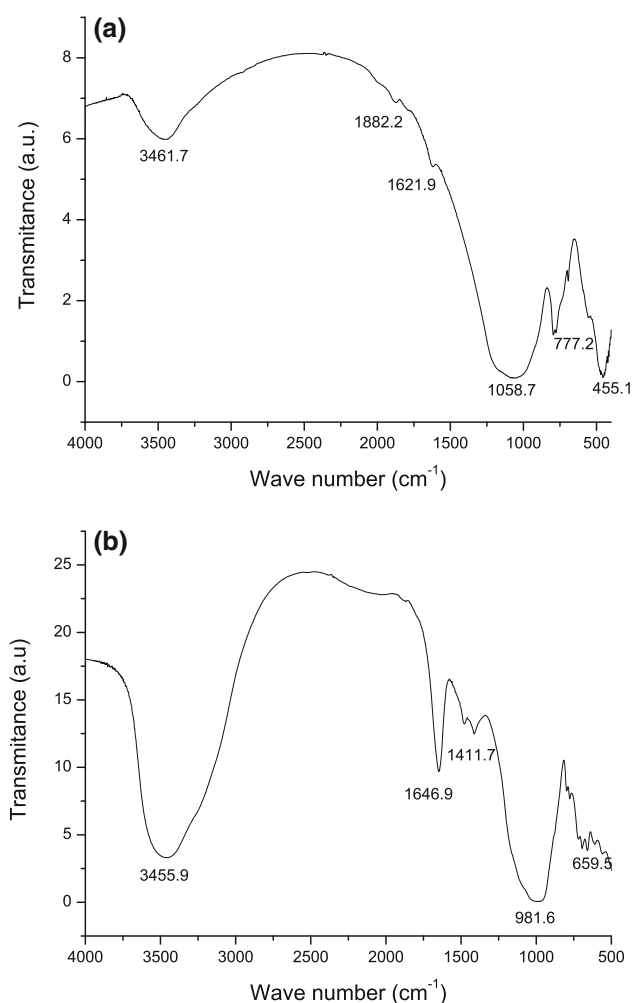The chemical composition of FA and ZM determined by X-ray fluorescence (XRF) is shown in Table 2. The

Table 2 Chemical composition of FA and ZM

Compound	FA (wt%)	ZM (wt%)
SiO$_2$	42.4	40.9
Al$_2$O$_3$	17.5	24.4
Fe$_2$O$_3$	6.38	11.7
Na$_2$O	1.18	10.9
CaO	1.09	5.03
K$_2$O	2.82	2.31
TiO$_2$	0.868	1.60
SO$_3$	0.400	1.26
MgO	0.539	1.07
ZnO	0.181	0.300
AsO$_3$	0.178	–
SiO$_2$/Al$_2$O$_3$	2.42	1.68

materials were characterized mainly as silica, alumina, iron oxide and sodium oxide. A significant amount of Na element is incorporated in the zeolitic product due to the hydrothermal treatment with NaOH solution.

The Fig. 2 compares spectra of FA and ZM. Spectrum (Fig. 2a) of the original FA possesses three absorption bands at 1058.7, 777.2 and 455.1 cm^{-1}. The 1058.7 and 455.1 cm^{-1} bands are due the asymmetric stretching and the bending vibration modes of T–O bands, respectively (where T = Si or Al). The 777.2 cm^{-1} band is assigned to the symmetric stretching vibration mode of O–T–O groups [24, 25]. The band at 1058.7 cm^{-1} in the FTIR spectrum of FA became sharper and shifted to lower frequency (981.6 cm^{-1}) in the FTIR spectrum of ZM (Fig. 2b) indicating the formation of a new product that is associated with the dissolution of the fly ash amorphous phase in the strong alkaline activation solution [26]. A broad intense OH stretching band and a weaker H–O–H deformation band were observed at 3461.7 and 1621.9 cm^{-1} in the FA spectrum and, 3455.9 and 1646.9 cm^{-1} in the ZM spectrum; the appearance of these bands define H–O–H deformation generally regarded to be indicative of the presence of a hydrated compound whose constitutional water is tightly bound to the molecular structure of the compound [27].
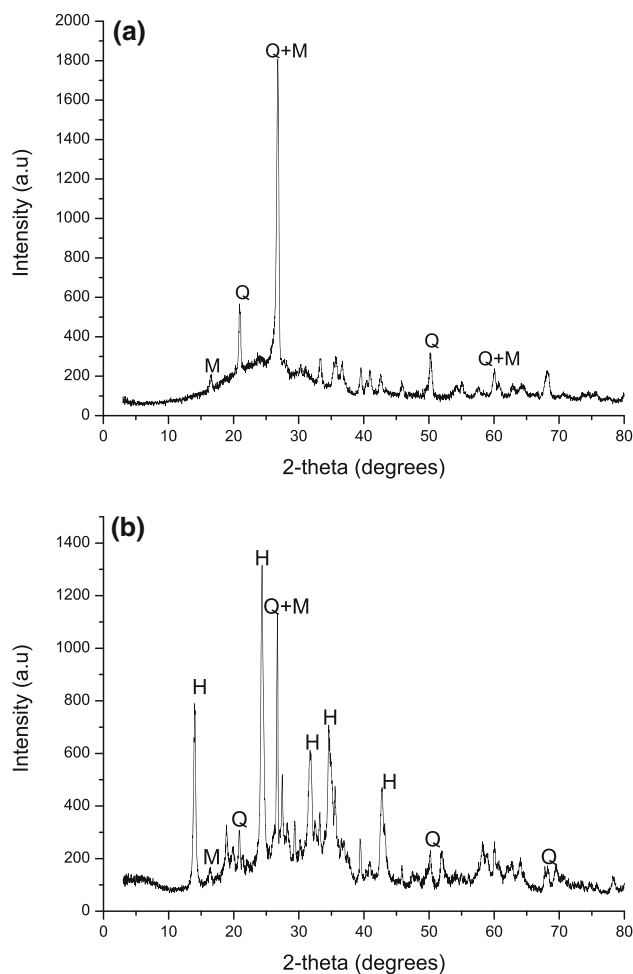
The FA pattern XRD (Fig. 3a) shows Cu Kα peaks at 20.9°, 26.6°, 50.1°, 67.9° positions which using the ICDD pattern data base indicated the predominant presence of quartz (ICDD 001-0649). The presence of the small peaks at 16.7°, 26.2°, 60.1° (ICDD 002-0430) could represent the presence of some amount of mullite. XRD analyses of ZM (Fig. 3b) indicated that NaOH hydrothermal treatment predominantly led to the formation of hydroxy-sodalite (ICDD 011-0401), whose chemical formula is Na$_4$Al$_3$Si$_3$O$_{12}$(OH).

Fig. 2 FTIR spectra of **a** FA and **b** ZM

Fig. 3 DRX diffractometers of **a** FA and **b** ZM (Q = quartz; M = mullite; H = hydroxysodalite)

Effect of contact time and of initial dye concentration

The relation between removal of IC and time with the adsorbents were studied to verify the rate of dye removal. As seen in the Fig. 4, lowest concentration showed the highest % removed IC and, the efficiency of dye removal was increased as the agitation time increased. The removal decreased from 100 to 84% by increasing FA concentrations from 4.4 to 14.7 mg L^{-1} (Fig. 4a), whereas when using ZM as adsorbent the removal was decreased from to 95 to 90% with concentrations from 3.6 to 11.0 mg L^{-1} (Fig. 4b). Dye adsorption equilibrium was established faster with FA which required 45 min whereas with ZM it was necessary 240 min to attain the equilibrium. These equilibrium times were used in all subsequent adsorption tests. The adsorption curves are smooth and continuous suggesting the possible of monolayer coverage of the IC on the adsorbents surfaces [13, 28]. The rapid adsorption at the much slower initial contact time for FA is probably due to the facility for dye molecules to reach the available surface sites than for ZM.

Kinetic study

In order to investigate the adsorption processes of IC onto adsorbents, pseudo-first order and pseudo-second order kinetic models were applied to the experimental data.

The linearized form of the pseudo-first order rate equation by Lagergren is given by Eq. 2:

$$\log(q_e - q_t) = \log q_e - \frac{k_1 t}{2.303} \qquad (2)$$

where q_t is the amount of dye adsorbed at time t (mg g^{-1}), q_e is the adsorption capacity at equilibrium (mg g^{-1}), k_1 is the equilibrium rate constant of pseudo-first order (min^{-1}) and, t is the contact time (min). Values of k_1 were obtained from the slopes of the linear plots of $\log(q_e - q_t)$ versus t, as shown in Fig. 5.

The intercept of the straight line plots of $\log(q_e - q_t)$ against t should be equal $\log(q_t)$. However, if the intercept does not equal q_t, then the reaction is not likely to be a first order reaction even this plot has high determination coefficient with the experimental data [7].
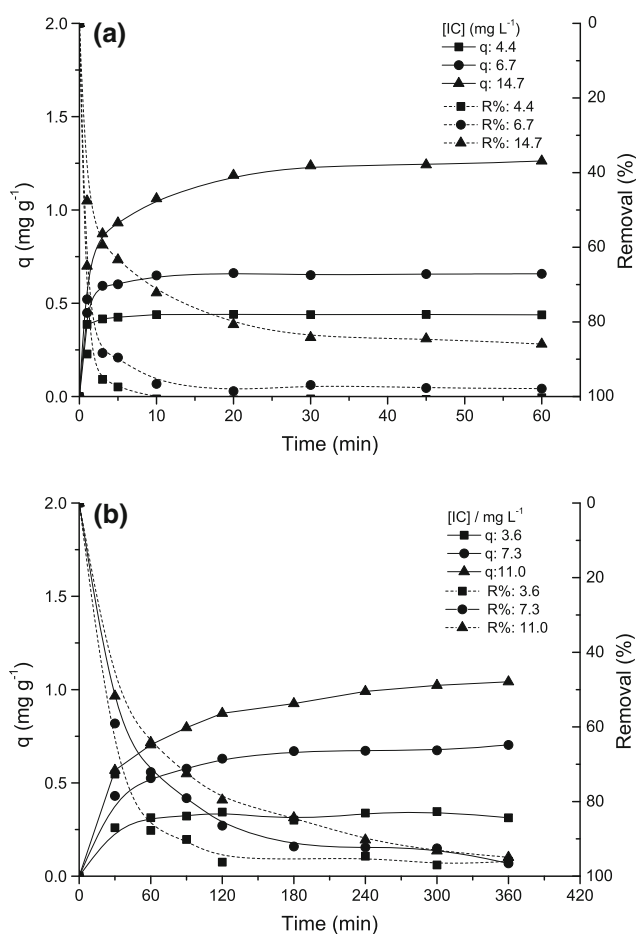
Fig. 4 Effect of time and initial concentration on removal of IC by a FA and b ZM

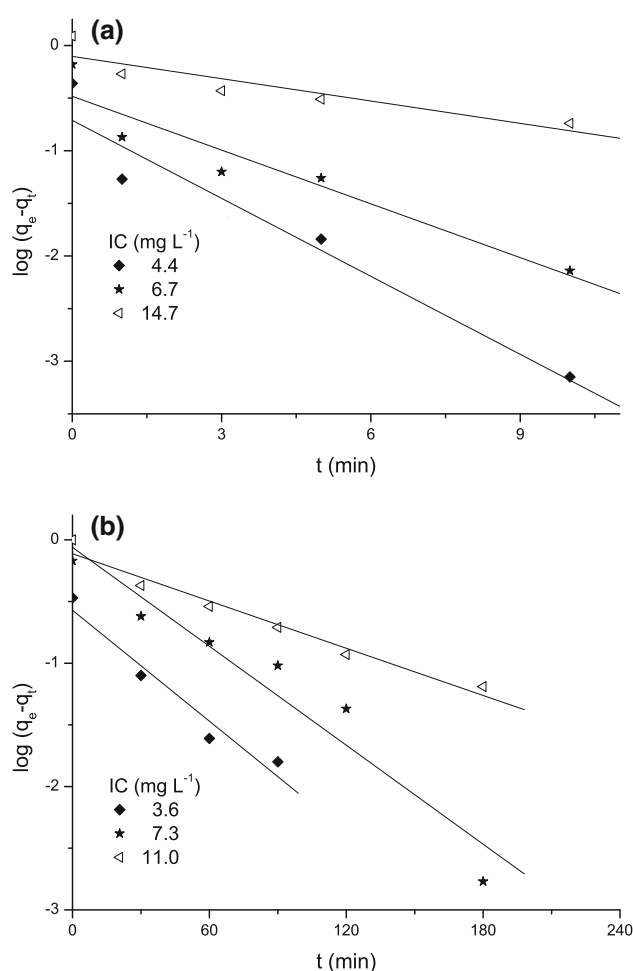Fig. 5 Pseudo-first order adsorption kinetics of IC onto a FA and b ZM

The experimental q_e values (Table 3) did not agree with the calculated ones obtained from the linear plots, indicating that the pseudo-first order model does not reproduce the adsorption kinetics of IC onto FA and ZM.

The linear form of pseudo-second order kinetic model [29] is expressed by Eq. 3:

$$\frac{t}{q_t} = \frac{1}{k_2 q_e^2} + \frac{1}{q_e} t \qquad (3)$$

where q_t is the amount of dye adsorbed at time t (mg g^{-1}), q_e is the adsorption capacity at equilibrium (mg g^{-1}), k_2 is the equilibrium rate constant of pseudo-second order adsorption (g mg^{-1} min^{-1}). By the straight lines plots of t/q_t against t for FA (Fig. 6a) and for ZM (Fig. 6b) was possible to calculate the values of k_2 from the intercepts and, q_e from the slopes.

The k_2 and q_e determined from the model are presented in Table 3 along with the corresponding determination coefficients. The values of the calculated and experimental q_e are close to FA and also to ZM, and the calculated determination coefficients (R_2^2) are also very close to unity. Hence, the pseudo-second order model better represented

the adsorption kinetics. It is also observed from Table 3 that the k_2 constant value decreases with increasing initial IC concentration for both adsorbents. This behavior can be attributed to the lower competition for the adsorption surface sites at lower concentration. At higher concentrations, the competition for the surface active sites will be high and, thus lower adsorption rates are obtained [30]. Similar data had been observed in the adsorption of IC by rice husk ash [31].

The prediction of the rate-limiting step is an important consideration since the adsorbate transport from the solution phase to the surface of the adsorbent particles may occur in one or more steps [31]. The possibility of intraparticle diffusion affecting the adsorption process was investigated by using the intraparticle diffusion model from Weber and Morris [32] following the Eq. 4:

$$q_t = k_{id} t^{1/2} + C \qquad (4)$$

where k_{id} is the intraparticle diffusion rate constant (mg g^{-1} min$^{-1/2}$), and C is the intraparticle diffusion constant (mg g^{-1}). The constants k_{id} and C can be

Table 3 Pseudo-first order and pseudo-second order parameters for IC adsorption onto FA and ZM

Adsorbent	Pseudo-first order model					Pseudo-second order model		
	IC (mg L^{-1})	q_e exp (mg g^{-1})	k_1 ($\times 10^{-2}$ min^{-1})	q_e calc (mg g^{-1})	R_1^2	k_2 (g mg^{-1} min^{-1})	q_e calc (mg g^{-1})	R_2^2
FA	4.4	0.440	56.9	0.194	0.925	25.4	0.439	0.999
	6.7	0.656	39.2	0.329	0.906	5.17	0.661	0.999
	14.7	1.24	16.3	0.788	0.823	0.489	1.29	0.999
ZM	3.6	0.338	3.45	0.269	0.953	0.104	0.329	0.990
	7.3	0.672	3.09	0.870	0.931	0.587×10^{-2}	0.740	0.999
	11.0	0.990	1.47	0.771	0.966	0.240×10^{-2}	1.14	0.999
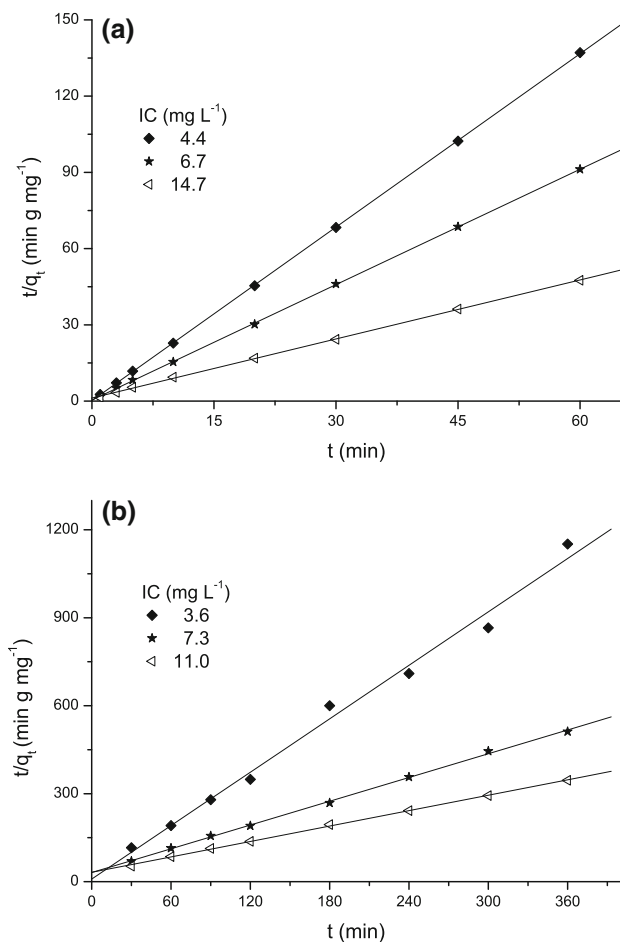
Fig. 6 Pseudo-second order adsorption kinetics of IC onto **a** FA and **b** ZM

obtained, respectively, from the slope and intercept of the plot of q_t versus $t^{1/2}$. The relative values of C give an idea about the boundary layer thickness, i.e., the larger the intercept value, the greater the boundary layer effect [33–35]. The plots (Fig. 7) show that there are not linearity over the whole time indicating that more than one step is controlling the adsorption process [31]. The first step (not in the plot), the external surface adsorption is observed from 0 to 1 min for FA (Fig. 7a) and, from 0 to 30 min for ZM

(Fig. 7b). Then the intraparticle diffusion control is attained and continues from 1 to 10 min for FA and, from 30 to 120 min for ZM. Finally, the final equilibrium adsorption (step 3) starts from 10 min to FA, and 120 min to ZM in the IC adsorption process [36].

It is observed from Table 4 that the C values increase with increasing IC initial concentrations, implying that the boundary layer diffusion mechanism becomes more significant when the dye concentration increases [30].

Adsorption isotherms

In adsorption in a solid–liquid system, the distribution ratio of the solute between the liquid and the solid phases is a measure of the position of equilibrium. The preferred form of depicting this distribution is to express the quantity q_e as a function of C_e at a fixed temperature and an expression of this type is termed an adsorption isotherm [37].

The analysis of the isotherm data is important to develop an equation which accurately represents the results and which could be used for design purposes [7]. Several adsorption isotherm equations are available and the two most used are Langmuir and Freundlich isotherms. The data obtained from the isotherm studies were tested for applicability to these two isotherm models.

The Langmuir isotherm assumes that the sorption takes place at specific homogeneous sites within the adsorbent [34]. The linear form of Langmuir isotherm is represented by the Eq. 5:

$$\frac{C_e}{q_e} = \frac{1}{Q_0 b} + \frac{C_e}{Q_0} \tag{5}$$

where C_e is the equilibrium concentration (mg L^{-1}), q_e the amount adsorbed at equilibrium (mg g^{-1}), Q_0 the adsorption capacity (mg g^{-1}) and, b is the energy of adsorption (Langmuir constant, L mg^{-1}). The values of Q_0 and b were calculated from the slope and intercept of the linear plots $C_e q_e^{-1}$ versus C_e which give a straight line of slope $1/Q_0$ that corresponds to complete monolayer coverage (mg g^{-1}) and the intercept is $1/Q_0 b$ (Figs. 8a, 9a). The experimental results fit the linearized Langmuir isotherm
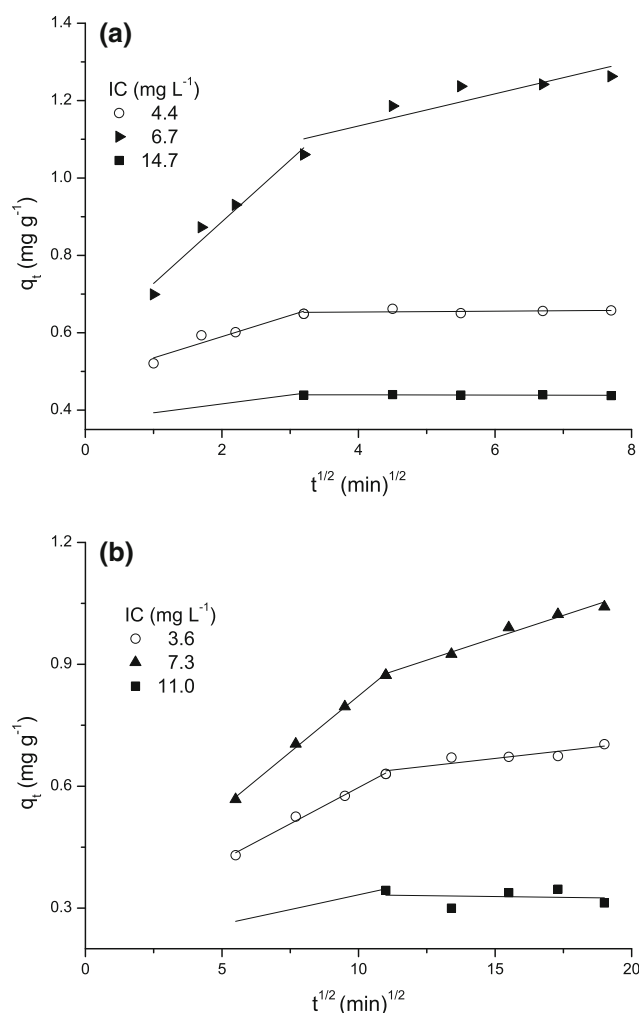
Fig. 7 Intraparticle diffusion plot for adsorption of IC onto **a** FA and **b** ZM

Table 4 Intraparticle diffusion constants for IC adsorption onto FA and ZM

Adsorbent	IC (mg L^{-1})	C (mg g^{-1})	k_{id}[a] (mg g^{-1} min$^{-1/2}$)	R^2_{id}
FA	4.4	0.370	0.0229	0.912
	6.7	0.480	0.0549	0.924
	14.7	0.568	0.159	0.965
ZM	3.6	0.187	0.0145	0.926
	7.3	0.240	0.0357	0.993
	11.0	0.269	0.0554	0.997

[a] Second step

for IC adsorption in both adsorbents over the investigated concentration range and the determination coefficients can be seen from Table 5. The values close to the unity for the determination coefficients support the assumption that the adsorption process follows the Langmuir model.

The Freundlich isotherm is derived by assuming a heterogeneous surface with a non-uniform distribution of heat
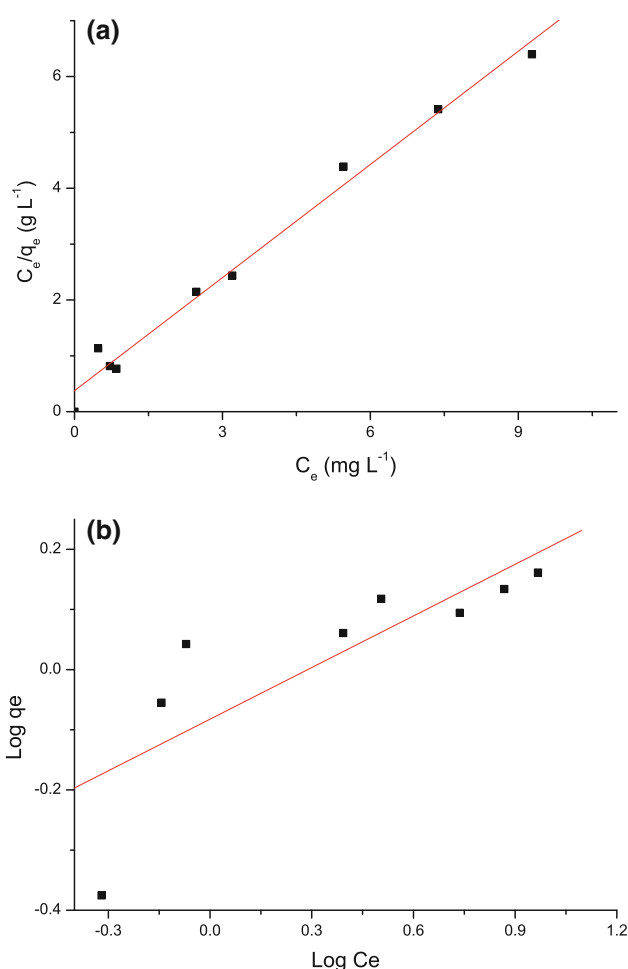
Fig. 8 a Langmuir isotherm and **b** Freundlich isotherm plot of adsorption of IC onto FA

of adsorption over the surface [38]. The logarithmic form is shown as Eq. 6:

$$\log q_e = \log K_F + \frac{1}{n} \log C_e \tag{6}$$

where K_F [(mg g^{-1} (L mg^{-1})$^{1/n}$)] and n are the Freundlich constants related to adsorption capacity and adsorption intensity of adsorbents, respectively. They were calculated from the intercept and slope of the plot log q_e versus log C_e (Figs. 8b, 9b).

The isotherm constants and determination coefficients calculated for Langmuir and Freundlich equations are given in Table 5. The experimental results do not fit the linearized Freundlich isotherm for both adsorbents over the investigated concentration range since the determination coefficients are far from the unity.

The FA and ZM have good potential to be used as adsorbent for the removal of indigo carmine from water. Similar behavior and result were observed by Brito et al. [39] when investigated the adsorption of IC onto Brazil nut shells.
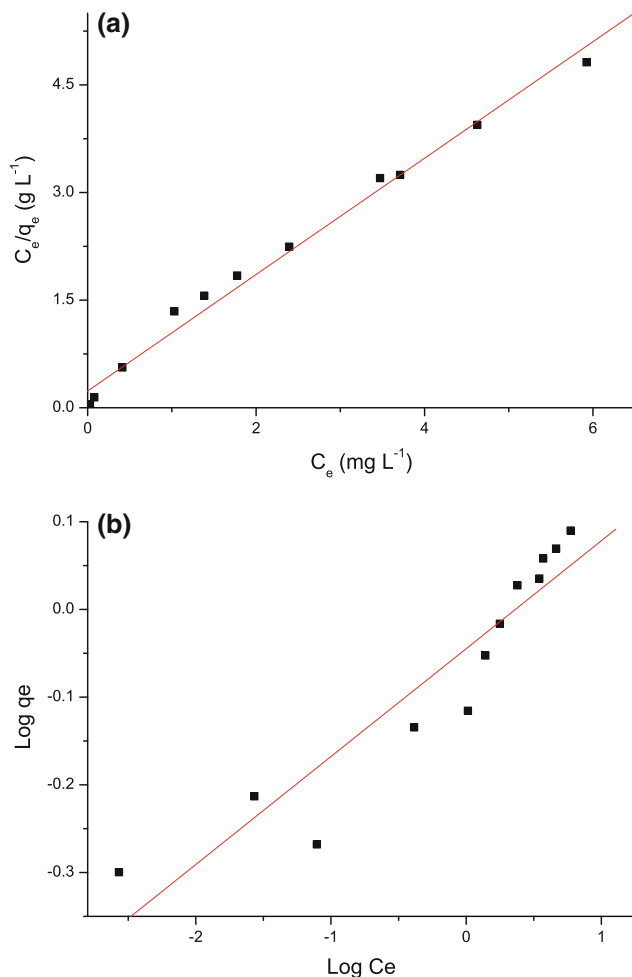
Fig. 9 a Langmuir isotherm and **b** Freundlich isotherm plot of adsorption of IC onto ZM

Table 5 Langmuir and Freundlich parameters for the adsorption of IC onto FA and ZM

Adsorbent	Langmuir			Freundlich		
	Q_0 (mg g^{-1})	b (L mg^{-1})	R^2	K_F[a]	n	R^2
FA	1.48	1.80	0.987	0.82	3.50	0.654
ZM	1.23	3.47	0.988	0.90	8.13	0.882

[a] [(mg g^{-1} (L mg^{-1})$^{1/n}$)]

Leaching and solubilization tests in ZM

The fly ash composition varies as a function of the coal source, but is generally enriched in a number of trace elements which may potentially become bio-available in environment applications [8]. Fly ashes trace elements analysis from Figueira Power Plant carried out by Depoi et al. [9] demonstrated that the average concentrations of some elements (As, Cd, Mo, Pb, Tl, U, Zn, and Hg) were of environmental concern since they are higher than in other Brazilian coals which in turn are, in general, similar to the

Table 6 Chemical elements in the adsorbents analyzed by INAA

Element	FA[a] (µg g^{-1})	ZM[a] (µg g^{-1})
As	1627 ± 48	29 ± 5
Co	21.5 ± 2.9	16.5 ± 0.2
Fe	77194 ± 32407	46727 ± 819
La[b]	114 ± 1	82 ± 16
Mo[b]	672 ± 14	368 ± 84
Na	9862 ± 174	69382 ± 20299
Sb	20.5 ± 0.1	4.2 ± 0.5
Sc	32.8 ± 4.4	23.0 ± 0.1
Sm	33.6 ± 1.6	22.0 ± 5.4
Th	533 ± 81	383 ± 6
U	345 ± 1	225 ± 43
Zn	2318 ± 321	1468 ± 53

[a] Mean and standard deviation of two determinations

[b] Elements that can be fission products

mean for coals from other countries. During the fly ash zeolitization these harmful elements dissolves into the alkaline solution, and are not incorporated into zeolites [40]. Therefore, before using the zeolitic material synthesized from fly ash in the water treatment, trace analyses of some elements were carried out in the FA and in the ZM in order to confirm the decrease of these elements during the zeolite synthesis process. The mean value concentration and standard deviation obtained using INAA are presented in Table 6.

A considerable reduction in the elements contents was attained in the fly ash zeolitization, as arsenic that decreased almost 98%. Only sodium was higher in the ZM, what was expected since NaOH solution works as an activator during the hydrothermal process.

Then, a ZM sample was submitted to leaching and solubilization tests [22, 23] for solid waste classification according to Brazilian regulation. Elements listed in the F annex of the ABNT norm [41] were analyzed and classified according to the toxicity by leaching of elements. Residues that present leaching concentration of elements above indexes are considered *Class I*, "hazardous waste". For results under index limits, samples are considered *Class II*, "non-hazardous waste". The Table 7 presents the analytical results for elements found in the extracts from leaching assay.

As the ZM was considered as residue *Class II*, non-hazardous waste, a solubilization test must be carried out in *Class II* samples to determine if non-hazardous elements are soluble in water for further defining *Class II* "inert" or "non-inert" waste. Elements listed in the G annex of the ABNT norm [41] were analyzed and classified according to the toxicity by solubilization of elements. The Table 8

Table 7 Concentration of elements leachated from ZM and the allowed limit values

Element	ZM[a] (mg L^{-1})	ABNT-NBR 10004 (mg L^{-1})
As	0.027 ± 0.001	1.0
Ba	0.336 ± 0.001	70.0
Cd	0.017 ± 0.001	0.5
Pb	0.010 ± 0.001	1.0
Cr	0.026 ± 0.001	5.0
Hg	<0.0008	0.1
Se	0.002 ± 0.0001	1.0

[a] Mean and standard deviation of three determinations

presents the analytical results for elements found in the extracts from solubilization assay.

The concentrations of Al, As, Pb, Fe and Na were superior to the allowed limit values to the solubilization assay, then according to the norm, ZM is classified as residue *Class II* "non-inert", i.e., non-hazardous and non-inert.

As the concentrations of elements are, in general, highest in the fly ashes from Figueira, zeolite synthesis with fly ash from other power plants from Brazil should be made in order to verify if the toxic elements could be removed or mobilized during the zeolitization.

Besides the concern with the pollution caused by FA and ZM to the environment, there is also a greater awareness about the quality of final water after the treatment with these adsorbents. An investigation demonstrated that acute toxicological studies with *Daphnia similis* done with the water obtained after the treatment with the same FA and ZM for reactive remazol red RB dye removal caused 100% organisms death when the adsorbent in the adsorption process was the FA. When the ZM was the adsorbent and the treated water was neutralized (pH of about 7) acute toxicological studies with *D. similis* demonstrated that the toxicity was eliminated [42]. Similar tests should be done with the indigo carmine.

Conclusion

The present study showed that is possible to convert fly ash into zeolitic material by alkaline hydrothermal treatment. The X-ray diffraction analysis demonstrated it predominantly to be hydroxy-sodalite. This zeolite synthesized from fly ash is a promising adsorbent for removal the anionic dye indigo carmine. The pseudo-second order model provides the best correlation of the experimental data and intraparticle diffusion is involved in the adsorption process, but it is not the only rate-limiting step. The equilibrium data fit with the Langmuir isotherm. The adsorption capacity for ZM was found to be 1.23 mg g^{-1}.

Table 8 Concentration of elements solubilized from ZM and the allowed limit values

Element	ZM[a] (mg L^{-1})	ABNT-NBR 10004 (mg L^{-1})
Al	2.67 ± 0.03	0.2
As	8.40 ± 0.10	0.01
Ba	0.023 ± 0.001	0.7
Cd	0.0006 ± 0.0001	0.005
Pb	0.033 ± 0.001	0.01
Cu	<0.020	2.0
Cr	0.041 ± 0.001	0.05
Fe	1.54 ± 0.02	0.3
Mn	0.013 ± 0.001	0.1
Hg	<0.0008	0.001
Se	0.001 ± 0.0001	0.01
Na	624 ± 8	200.0
Zn	0.080 ± 0.001	5.0

[a] Mean and standard deviation of three determinations

Laboratory leaching and solubilization tests conducted to classify the zeolitic material (as if was a waste solid residue) according to the Brazilian regulation classified it as a residue non-hazardous and non-inert. Although the fly ash used in this study demonstrated to have a little better adsorption capacity (1.48 mg g^{-1}) than zeolitic material, more research is required to assess all the risk of using it as adsorbent to the environment because leaching tests with water showed that several elements are extracted in high proportions.

References

1. Ammar S, Abdelhedi R, Flox C, Arias C, Brillas E (2006) Electrochemical degradation of the dye indigo carmine at boron-doped diamond anode for wastewaters remediation. Environ Chem Lett 4:229–233
2. Mittal A, Mittal J, Kurup L (2006) Batch and bulk removal of hazardous dye, indigo carmine from waste water through adsorption. J Hazard Mater B 137:591–602
3. Barka N, Assabbane A, Nounah A, Ichou YA (2008) Photocatalytic degradation of indigo carmine in aqueous solution by TiO$_2$-coated non-woven fibres. J Hazard Mater 152:1054–1059
4. Othman I, Mohamed RM, Ibrahem FM (2007) Study of photocatalytic oxidation of indigo carmine dye on Mn-supported TiO$_2$. J Photochem Photobiol A 189:80–85
5. Das D, Sureshkumar MK, Koley S, Mithal N, Pillai CGS (2010) J Radioanal Nucl Chem 285:447
6. Hassan HS, Attallah MF, Yakout SM (2010) Sorption characteristics of an economical sorbent material used for removal of radioisotopes of cesium and europium. J Radioanal Nucl Chem 286:17–26

7. Ho YS, McKay G (1998) Sorption of dye from aqueous solution by peat. Chem Eng J 70:115–124

8. Levandowski J, Kalkreuth WD (2009) Chemical and petrographical characterization of feed coal, fly ash and bottom ash from the Figueira Power Plant, Paraná, Brazil. Int J Coal Geol 77:269–281

9. Depoi FS, Pozebon D, Kalkreuth WD (2008) Chemical characterization of feed coals and combustion-by-products from Brazilian power plants. Int J Coal Geol 76:227–236

10. Meawad AS, Bojinova DY, Pelovski YG (2010) An overview of metals recovery from thermal power plant solid wastes. Waste Manage 30:2548–2559

11. Polic PS, Ilic MR, Popovic AR (2005) Environmental impact assessment of lignite fly ash and its utilization products as recycled hazardous wastes on surface and ground water quality. Handb Environ Chem. doi:10.1007/b11733

12. Woolard CD, Petrus K, Van der Horst M (2000) The use of a modified fly ash as an adsorbent for lead. Water SA 26:531–536

13. Fungaro DA, Izidoro JC (2006) Remediação de drenagem ácida de mina usando zeólitas sintetizadas a partir de cinzas leves de carvão. Quím Nova 29:735–740 (in Portuguese with English abstract)

14. Fungaro DA, Graciano JEA (2007) Adsorption of zinc ions from water using zeolite/iron oxide composites. Adsorpt Sci Technol 10:729–740

15. Querol X, Moreno N, Umaña JC, Alastuey A, Hernández E, López-Soler A, Plana F (2002) Synthesis of zeolites from coal fly ash: an overview. Int J Coal Geol 50:413–423

16. Carvalho TEM, Fungaro DA, Izidoro JC (2010) Adsorção do corante reativo laranja 16 de soluções aquosas por zeólita sintética. Quím Nova 33:358–363 (in Portuguese with English abstract)

17. Fungaro DA, Grosche LC, Pinheiro AS, Izidoro JC, Borrely SI (2010) Adsorption of methylene blue from aqueous solution on zeolitic material and the improvement as toxicity removal to living organisms. Orbital 2:235–247

18. Fungaro DA, Bruno M, Grosche LC (2009) Adsorption and kinetic studies of methylene blue on zeolite synthesized from fly ash. Desalin Water Treat 2:231–239

19. Wang CJ, Li J, Wang L, Sun X, Huang J (2009) Adsorption of dye from wastewater by zeolites synthesized from fly ash: kinetic and equilibrium studies. Chin J Chem Eng 17:513–521

20. Wang S, Soudi M, Li L, Zhu ZH (2006) Coal ash conversion into effective adsorbents for removal of heavy metals and dyes from wastewater. J Hazard Mater B 133:243–251

21. Henmi T (1987) Synthesis of hydroxy-sodalite ("zeolite") from waste coal ash. Soil Sci Plant Nutr 33:517–522

22. Brazil, Technical Standard (2004) Associação Brasileira de Normas Técnicas, ABNT NBR 10005. Procedure for obtention leaching extract of solid wastes (in Portuguese)

23. Brazil, Technical Standard (2004) Associação Brasileira de Normas Técnicas, ABNT NBR 10006. Procedure for obtention solubilizing extract of solid wastes (in Portuguese)

24. Ojha K, Pradhan NC, Samanta AN (2004) Zeolite from fly ash: synthesis and characterization. Bull Mater Sci 27:555–564

25. Tanaka H, Matsumara S, Hino R (2004) Formation process of Na–X zeolites from coal fly ash. J Mater Sci 39:1677–1682

26. Criado M, Palomo A, Fernández-Jiménez A (2005) Alkali activation of fly ash, Part 1, effect of curing conditions on the carbonation of the reaction products. Fuel 84:2048–2054

27. Fernández-Jiménez A, Palomo A, Vasquez T, Vallepu R, Terai T, Ikeda K (2008) Alkaline activation of blends of metakaolin and calcium aluminate cement, Part I, strength and microstructural development. J Am Ceram Soc 91:1231–1236

28. Tor A, Cengeloglu Y (2006) Removal of congo red from aqueous solution by adsorption onto activated red mud. J Hazard Mater B 138:409–415

29. Ho YS, McKay G (1999) Pseudo-second order model for sorption processes. Process Biochem 34:451–465

30. Chen H, Zhao J, Dai G (2011) Silkworm exuviae—a new non-conventional and low-cost adsorbent for removal of methylene blue from aqueous solutions. J Hazard Mater 186:1320–1327

31. Lakshmi UR, Srivastava VC, Mall ID, Lataye DH (2009) Rice husk ash as an effective adsorbent: evaluation of adsorptive characteristics for indigo carmine dye. J Environ Manage 90:710–720

32. Weber WJ, Morris JC (1963) Kinetics of adsorption carbon from solutions. J Sanit Eng Div ASCE 89:31–60

33. Nemr AE, Abdelwahab O, El-Sikaily A, Khaled A (2009) Removal of direct blue-86 from aqueous solution by new activated carbon developed from orange peel. J Hazard Mater 161:102–110

34. Zou W, Zhao L, Han R (2011) Adsorption characteristics of uranyl ions by manganese oxide coated sand in batch mode. J Radioanal Nucl Chem 288:239–249

35. Kannan K, Sundaram MM (2001) Kinetics and mechanism of removal of methylene blue by adsorption on various carbons—a comparative study. Dyes Pigm 51:25–40

36. Xia C, Jing Y, Jia Y, Jun M, Yue D, Ma J, Yin X (2011) Adsorption properties of congo red from aqueous solution on modified hectorite: kinetic and thermodynamic studies. Desalination 265:81–87

37. Weber WJ Jr (1972) In: Weber WJ Jr (ed) Physicochemical processes for water quality control. Wiley-Interscience, New York

38. Mall ID, Srivastava VC, Agarwal NK, Mishra IM (2005) Removal of congo red from aqueous solution by bagasse fly ash and activated carbon: kinetic study and equilibrium isotherm analyses. Chemosphere 61:492–501

39. Brito SMO, Andrade HMC, Soares LF, Azevedo RP (2010) Brazil nut shells as a new biosorbent to remove methylene blue and indigo carmine from aqueous solutions. J Hazard Mater 174:84–92

40. Inada M, Eguchi Y, Enomoto N, Hojo J (2005) Synthesis of zeolite from coal fly ash with different silica–alumina composition. Fuel 84:299–304

41. Brazil, Technical Standard (2004) Associação Brasileira de Normas Técnicas, ABNT NBR 10004. Classification of solid residues (in Portuguese)

42. Magdalena CP (2010) Adsorption of reactive remazol red RB dye of aqueous solution using zeolite of the coal ash and evaluation of acute toxicity with *Daphnia similis*. http://pelicano.ipen.br/PosG30/TextoCompleto/Carina%20Pitwak%20Magdalena_M.pdf. Accessed 14 Apr 2011 (in Portuguese with English abstract)